

Experimental study on the accuracy and surface quality of printed versus machined holes in PEI Ultem 9085 FDM specimens

Giovanni Gómez-Gras, Marco A. Pérez, Jorge Fábregas-Moreno and Guillermo Reyes-Pozo
IQS School of Engineering, Universitat Ramon Llull, Barcelona, Spain

Abstract

Purpose – This paper aims to investigate the quality of printed surfaces and manufacturing tolerances by comparing the cylindrical cavities machined in parts obtained by fused deposition modeling (FDM) with the holes manufactured during the printing process itself. The comparison focuses on the results of roughness and tolerances, intending to obtain practical references when making assemblies.

Design/methodology/approach – The experimental approach focuses on the comparison of the results of roughness and tolerances of two manufacturing strategies: geometric volumes with a through-hole and the through-hole machined in volumes that were initially printed without the hole. Throughout the study, both alternates are explained to make appropriate recommendations.

Findings – The study shows the best combinations of technological parameters, both machining and three-dimensional printing, which have been decisive for obtaining successful results. These conclusive results allow enunciating recommendations for use in the industrial environment.

Originality/value – This paper fulfills an identified need to study the dimensional accuracy of the geometries obtained by additive manufacturing, as no experimental evidence has been found of studies that directly address the problem of the FDM-printed part with geometric and dimensional tolerances and desirable surface quality for assembly.

Keywords Additive manufacturing, Surface roughness, Machining, Fused deposition modeling, Tolerances, 3D printing, Roughness

Paper type Research paper

1. Introduction

The manufacturing landscape is continuously changing. Some drivers of this change are the demand for more efficient technologies, faster adaptation to market needs and the requirement to extend product life to ensure more sustainable production. Combining these interests with customization, recycling and other socio-economic patterns, additive manufacturing (AM) stands out as one of the most promising innovations, with a high potential to change the distribution of manufacturing and position it in the revolutionary paradigm of Industry 4.0. AM has been identified as having the potential to provide numerous sustainability advantages. These benefits include the generation of less waste during manufacture, the ability to create lightweight components and the optimization of material and energy consumption during use. Additionally, as there is no need for specific molds or tools, delays between design and manufacture could be reduced. *Ituarte et al. (2015)* performed a comparative study with three different AM technologies, demonstrating that it is possible to reduce costs and time to market. However, in all cases, surface quality was the most challenging requirement to satisfy, especially the flatness and the distance hole.

The expanded range of applications introduces the possibility of using three-dimensional (3D) printed parts for

assemblies with metal components or other materials. This fact poses a problem concerning dimensional and geometrical quality, which has not yet been addressed in depth by the scientific community. Accordingly, due to its significant industrial interest, the main objective of this work is the study of Ultem® 9085 (PEI, Ultem) parts obtained by fused deposition modeling (FDM), which could become part of assemblies with other components. The aim is to provide relevant information on surface quality, dimensional accuracy and the fundamental differences between obtaining

© Giovanni Gómez-Gras, Marco A. Pérez, Jorge Fábregas-Moreno and Guillermo Reyes-Pozo. Published by Emerald Publishing Limited. This article is published under the Creative Commons Attribution (CC BY 4.0) licence. Anyone may reproduce, distribute, translate and create derivative works of this article (for both commercial and non-commercial purposes), subject to full attribution to the original publication and authors. The full terms of this licence may be seen at <http://creativecommons.org/licenses/by/4.0/legalcode>

This work has been partially funded by the Ministry of Science, Innovation and Universities through the project New Developments in Lightweight Composite Sandwich Panels with 3D Printed Cores (3DPC) – RTI2018-099754-A-I00 and by the RIS3CAT Llabor 3D Community co-financed by the Generalitat de Catalunya (ACCIÓ) through the project TRANSPORT, l'Obra Social "La Caixa" (grant number 2017-LC-08) and COMRDI16-1-0010 – (2017-2020). The authors are very grateful to Mercedes Peña and César Alquézar for their invaluable support during the test experiments.

Received 5 December 2019
Revised 29 May 2020
30 September 2020
Accepted 18 November 2020

The current issue and full text archive of this journal is available on Emerald Insight at: <https://www.emerald.com/insight/1355-2546.htm>



Rapid Prototyping Journal
27/11 (2021) 1–12
Emerald Publishing Limited [ISSN 1355-2546]
[DOI 10.1108/RPJ-12-2019-0306]

final printed parts or printed and subsequently machined parts using conventional manufacturing processes.

The success of AM and its adoption in the industrial sector lies in the ability to ensure that material and dimensional properties meet a defined quality standard and, in turn, maintain a competitive production cost. This fact implies that there must be confirmation of the intended properties through proper methodology, materials selection, optimization of production, adaptation to current environmental requirements and everything needed to transform the AM from rapid prototyping to industrial manufacturing. Nevertheless, for this transformation to occur, all the processes related to AM have to be studied and validated. In this sense, an interesting study is presented by Ford and Despeisse (2016), in which they approach this transformation from the perspective of sustainability as an industrial process. They propose four main categories that can achieve sustainability benefits for AM, adopting the life cycle perspective. Like other authors, they present their contribution to the transition toward a more sustainable industry as a significant advantage of additive manufacturing.

Evidence from current AM research reveals that surface quality is one of the most critical problems associated with 3D printing. Overall, studies agree that the quality of the parts obtained by AM is highly dependent on the control of the printing parameters. Generally, researchers have classified these problems into four categories: optimization of build orientation, layer thickness, fabrication parameters optimization and post-treatment. The build orientation and the layer thickness have been two of the most approached parameters in the scientific literature showing to be essential factors in determining the quality of the specimen surface. Vasudevarao et al. (2000) proposed an experimental design technique to determine the optimum surface, analyzing the effects of the build orientation, layer thickness, contour width, air gap and model temperature on the surface quality. The authors concluded that the layer thickness and the specimen orientation are the most critical parameters. One year later, Anitha et al. (2001) also made a study of the same parameters, revealing that layer thickness is the most influential. In a similar experimental approach, Vijay et al. (2011) concluded that for the construction orientation of 20° and 45°, the surface roughness value is directly proportional to the thickness of the layer and for orientation of 70°, the roughness value is inversely proportional. Specifically, the layer thickness parameter seems to be relevant for both dimensional quality and roughness.

However, to date, there is no consensus in the literature on which parameters are responsible for the surface results obtained in FDM-printed parts. Researchers agree that surface quality is a consequence of the combination of print parameters, and as many parameters are involved in the process, it is difficult to study all the possible interrelationships between them. An interesting study was carried out by Chang and Huang (2011), focused on the analysis of errors in printed profiles, addressing the study of the parameters from another perspective. They proposed a two-dimensional spiral model with 19 standard cylinders to evaluate the profile, which would be compatible with any printing process layer by layer. They conclude that the contour's width is the most significant factor, without ruling out the influence of the other factors. Most

authors agree that it is essential to consider the properties of the material used and the temperature at which the layers are deposited, to have depth knowledge of the influence of the technological parameters of AM and to predict the quality of the finish. As a partial conclusion, is highlighted the review made by Mohamed et al. (2015) which revealed how several scientific studies had been concerned with evaluating the mechanical properties and the quality of printed samples by FDM from different points of view, putting in common that there is a direct dependence on the handling of the printing parameters when it comes to getting the best results.

In addition to the above, an optimal configuration of manufacturing parameters to improve surface finish could compromise its structural performance. Consequently, several studies have examined the relationship between the printing parameters, particularly the printing angle so often used to determine the surface quality and their influence upon the mechanical properties. Nidagundi et al. (2015) presented a study in which they evaluated four response parameters: tensile strength, surface roughness, dimensional accuracy and manufacturing time. They concluded that the combination of parameters is key to the tensile strength of the specimens tested. Sood et al. (2010), also combining printing parameters, studied the tensile strength and two other response variables: bending and impact strength. They assert that the loss of resistance is due to the distortion within or between the layers. The authors concluded that to minimize length changes in the test part, a higher layer thickness (0.254 mm), a 0° orientation, the highest raster angle (60°), a medium raster width (0.4564 mm) and a maximum air gap (0.008 mm) is desirable. Concerning width changes, the best parameter selection was the raster angle 30° and the air gap 0.004 mm.

To minimize thickness changes, it was found that the best combination was the lowest value of layer thickness, orientation 0°, raster angle 0°, a higher value of raster width and a mean value of the air gap. Other researchers analyzed the impact of the type of raster pattern and the filling density on mechanical behavior (Forés-Garriga et al., 2020). The study presented by Fernandez-Vicente et al. (2016) evaluated the variables pattern and infill density for parts printed in ABS to compare their tensile strength. They showed that the infill density determines the changes in the resistance and that the different printing patterns only cause variations around 5%. The best combination was a rectilinear pattern with 100% infill.

Although tensile strength appears the parameter most studied in the literature (Bahrami et al., 2020), other mechanical properties such as flexural strength (Zandi et al., 2020) and creep (Salazar-Martín et al., 2018) have been investigated to verify the influence of print parameters and to analyze the extent to which it can be modified as a function of surface roughness (Sedighi et al., 2019). The study of Mohamed et al. (2017) concluded that the progressive yield stress varies directly with the thickness of the layer, the raster angle and the air gap and on the contrary, varies inversely with the width of the raster and the number of layers.

Another relevant conclusion of these studies is the influence of the support material on the surface finish. In this sense, the reduction of the amount of support led to an improvement in the surface finish (Chueca de Bruijn et al., 2020). The relevance of the build orientation is again evident, as the

amount of support is directly associated with that parameter. With the correct build orientation, the support material can be significantly reduced and the number of surfaces in contact with the support material is minimized. This fact suggests that the surface quality of non-contact faces is potentially better. If it were possible to dispense with the support material when printing, one of the elements that most negatively affects the final roughness of the specimens would be eliminated. However, this does not seem to be a viable option when it comes to manufacturing parts with complex geometries by FDM, so alternate solutions need to be investigated. In this direction, it is worth mentioning the work published by Galantucci *et al.* (2009) in which the authors propose reducing the density of the parts and optimizing them topologically, thus avoiding the use of support material in some regions of the specimens. Throughout the study, they propose alternate styles of construction, which could contribute to optimizing the use of the support material.

Other recent studies have addressed the dimensional accuracy achieved by AM technologies. For example, some authors have focused on dimensional analysis, flatness error and texture of surfaces obtained by 3D printing, as in the work of Nunez *et al.* (2015). The authors concluded that for ABS specimens, minimal errors were obtained with 100% fill density, higher dimensional accuracy was reached with a layer thickness of 0.254 mm, the best surface finish was achieved with a layer thickness of 0.178 mm and the minimum flatness error was made with a layer thickness of 0.178 mm.

While most studies have focused on obtaining the best combination of print parameters, other approaches investigated the post-printing treatments. According to some authors, the key to improving surface quality lies in the post-processing of printed parts, as specific configurations of print parameters can be detrimental to mechanical performance. In this sense, there seems to be general agreement on the three types of post-treatments (Chohan and Singh, 2017): machining processes, as shown by Pandey *et al.* (2003), chemical procedures, as studied by Galantucci *et al.* (2009, 2010) and heat treatments, as the work by Wang *et al.* (2016). More specifically, Galantucci *et al.* (2009, 2010) proposed surface improvements based on the chemical immersion of the printed parts in a dimethyl ketone-water solution and evaluating the mechanical properties of traction and bending between the treated and non-chemically treated parts. The results presented by Wang *et al.* (2016), showed that the appropriate thermal treatment conditions exert a positive influence on mechanical properties. Compared to the untreated parts, the tensile and compression strength increased by 25.4% and 52.2%, respectively.

Over the past years, some other methods for improving the finish of printed surfaces have been documented. For example, Pandey *et al.* (2003) stated that the problem of surface quality is especially critical in some regions of reduced accessibility. The authors proposed a semi-empirical model for evaluating the surface roughness of specimens obtained by fused deposition. The problem was approached by combining AM with the hot-cutting machining (HCM) method for material removal. With this hybrid system, the authors proved that roughness of $0.3 \mu\text{m}$ could be obtained with a confidence level of 87%. Singh *et al.* (2017) studied the problem of surface quality by post-processing through chemical exposure (acetone) through

the use of the steam straightening station (VSS). They validated the VSS method to improve the surface finish at the nano level with negligible dimensional deviations. On the same lines, other authors such as Tiwary *et al.* (2019) deepened on the effects of various types of pre-processing and post-processing on surfaces. They compared the variations in the surface quality of printed samples of acrylonitrile butadiene styrene, after having subjected them to steam smoothing, chemical treatments and sandpaper polishing. The results were compared, finding that chemical treatments provided the lowest roughness. Finally, Del Sol *et al.* (2019) have recently studied the idea of correcting the typical additive manufacturing errors using post-processing machining. The authors milled perimeter samples printed by FDM using up, down and front milling strategies and analyzed the surface quality with the response indicators R_a , R_z and R_{sm} . They observed that the average roughness was reduced 10 times and the dimensional accuracy increased to 50%.

In the reviewed literature, no evidence has been found of studies directly addressing the problem of FDM-printed parts with geometric and dimensional tolerances and desirable surface quality for assembly. The dimensional accuracy remains a central issue and a constraint on the industrial expansion of the AM technologies. Consequently, in this research, the dimensional accuracy of FDM printed parts is addressed, comparing two approaches: printing or machining the through-hole on FDM parts. Throughout the study, both alternates are explained to make appropriate recommendations.

2. Methodology

In this study, two differentiated strategies were set. The first consists of manufacturing solid FDM parts to be drilled, considering the machining's three fundamental parameters: the drilling diameter, the feed and the spindle speed, which provides the cutting speed. This approach allowed determining the optimum parameters by which the best surface and quality were obtained. The second strategy consists of printing FDM samples, including the holes, optimizing the fundamental parameters of FDM such as infill percentage, number of contours and building orientation. For both strategies, the overall dimensions of the specimens and the holes' diameters were preserved. Alternately, some reference parts were also printed under two printing conditions, solid and sparse, which were used to compare the resultant surfaces.

Based on these considerations, specimens were designed to meet all the methodology requirements. Once the printing and subsequent machining were completed, parts were subjected to surface roughness measurements, geometric and dimensional accuracy and visual inspection with microscope imaging.

3. Experimental approach

3.1 Parameters definition

The settings of experimental parameters are divided into three groups: parameters common to both strategies, parameters related to the drilling process and technological parameters for FDM printing.

3.1.1 Common parameters

To simplify the comparison task, the same hole diameters are used in both strategies. The three-hole diameters to be analyzed are 10 mm, 15 mm and 20 mm. The hypothesis behind this variation of the parameter is that horizontally printed holes, i.e. printed with a central hole axis parallel to the x-axis, can vary their shape more, as they are in contact with the support material whose filling density is not 100%. Therefore, it can leave more space for the variation of the shape originated by the contractions produced during the cooling. Moreover, for the machining strategy, the diameter affects the rate of material removal and in the case of the printed hole, the diameter affects the extraction of the support material. Thus, this parameter can affect the quality of the dimension and the interior surface.

3.1.2 Machining parameters

Three new drills intended and certified to machine polymers [1], coupled with a conventional milling machine, were used to make the through-holes. Three different cutting speeds were applied in accordance with the drill diameter, starting from the one recommended for thermoplastics by the drill manufacturer (30 m/min). The cutting speed is doubled and tripled to investigate the influence on roughness. Thus, the feed was set at three levels: 0.04 mm/rev, 0.08 mm/rev and 0.16 mm/rev. These values were considered suitable for the proposed tests.

3.1.3 Fused deposition modeling parameters

There are various parameters associated with additive manufacturing that can be related to the final results. The aim of this research is specifically the optimization of these parameters so that the minimum of necessary material is used.

As these are two printing strategies, the selection of parameters must also be differentiated. In samples that were subsequently machined, a fill density of 100% was set, i.e. solid samples; otherwise, the perforation would cause holes to appear on the surface. Furthermore, it is doubtful whether a less dense structure can withstand the stress inherent in the machining process. For the second group of models, the minimum material premise was followed. Accordingly, it was set one contour and 50% infill density.

For samples of both strategies, the raster angle was $\pm 45^\circ$ and the number of outer contours was set to one. This study also tested the effect of the build orientations, which were flat, edge and at 45° . Other parameters such as the raster and the contour width, were settled by the nozzle used (T16 with slice height of 0.254 mm), leading to a filament and raster width of 0.514 mm.

3.2 Factorial experiment design

A full factorial design was applied to identify the interaction of the parameters in each value combination. For machined samples, four factors (diameter, build direction, feed and cutting speed) were used with three levels each, which means a factorial design of 3^4 . In models with FDM-printed holes, two factors (diameter and build direction) were used with three levels each, which means a factorial design of 3^2 . In both cases, the significance level is $\alpha = 0.05$. Each level is encoded with an alphanumeric combination, as depicted in Table 1.

The complete code of a hole is, for example, D20FA1V1. In this case, its label stands for a machined hole with a diameter of 20 mm, built in a flat direction, machined with a feed of 0.04 mm/rev and a cutting speed of 30 m/min.

Table 1 Parameter coding system

Parameter (factor)	Machined samples Full-factorial* design 3^4		Hole-printed samples Full-factorial* design 3^2	
	Value (level)	Code	Value (level)	Code
Diameter (mm)	10	D10	10	D10
	15	D15	15	D15
	20	D20	20	D20
Build direction	Flat	F	Flat	F
	Edge	E	Edge	E
	45°	45	45°	45
Feed [mm/rev]	0.04	A1	–	–
	0.08	A2	–	–
	0.16	A3	–	–
Cutting speed [m/min]	30	V1	–	–
	60	V2	–	–
	90	V3	–	–

Note: *Significance level is $\alpha = 0.05$

3.3 Material and specimens

In this research, an engineering-grade thermoplastic was chosen, widely used in the production of functional prototypes, automotive parts and aeronautical components. Specifically, it is the high-performance polymer resin of the family of polyetherimides (PEI) known commercially as Ultem. Among the different ULTEM grades available on the market, this research is focused on 9085 grade because of its high strength-to-weight ratio, high thermal and chemical resistance and flame, smoke and toxicity classifications (FST) making it very attractive to the aerospace and transportation industry and, therefore, especially interest for this study.

Considering the parameters of the post-printing drilling strategy and its corresponding levels, each model had space for nine holes, which correspond with the combinations of these three levels: diameters, feed and cutting speeds. A total of nine parts were printed, three for each model in each of the three directions. The samples were manufactured in a Stratasys Fortus 400mc.

For the FDM-printed holes' strategy, three models were designed, but with only one hole for each diameter, maintaining a model height of twice the diameter. Each model was printed three times, considering the three-building orientations. Accordingly, a total of 12 volumes were produced, as shown in Figure 1. When the support was correctly removed, drilling was performed and each hole was machined according to previously established parameters. Figure 2 illustrates the appearance of the specimens once they were drilled.

Table 2 collects the resources associated with the manufacture of these specimens, under each of the described conditions. In this table, it is possible to recognize the essential differences in material volume and printed time due to the particularities of the proposed configurations. This critical data should also be taken into account when deciding on the optimal parameters.

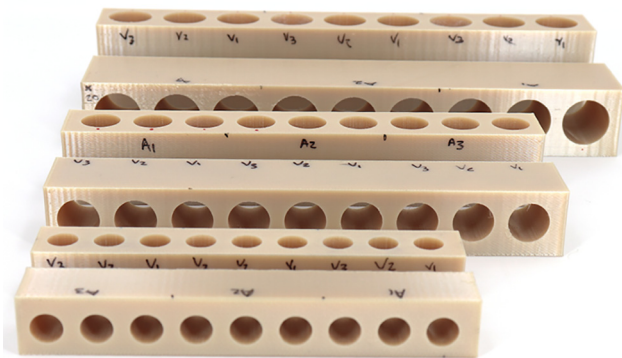
3.4 Dimensional tolerances

Three go/no-go gauges were used to verify the tolerance of the holes. According to Stratasys' recommendations regarding

Figure 1 Specimens with FDM-printed holes



Figure 2 Specimens with machined holes



manufacturing tolerances, the FDM process has a tolerance of ± 0.3 mm. Therefore, this is the reference taken to design gauges Figure 3. The upper and lower deviations of each gauge from the nominal diameters are shown in Table 3.

The dimension of each hole was measured using a centesimal precision micrometer in four locations, two in the top face and

Figure 3 Manufactured aluminum go/no-go gauges for verification



Table 3 Upper and lower deviations of each gauge from the nominal diameters (mm)

Nominal dimension	Top deviation	Lower deviation
20	20.30	19.70
15	15.30	14.70
10	10.30	9.70

two in the bottom face. One of the measures was made lengthwise regarding the main direction of the model and the other was made transversely. As there is no main direction in FDM hole specimens, measures were made considering the direction of the filaments so that they could be compared with the machined holes. The angle formed by the difference in dimension between the top and bottom was calculated, assuming that the deviation is linear. This angle was compared with the

Table 2 Resources associated with the FDM specimens manufacture

Specimens	Sample	Orientation	Part interior style	Hole diameter (mm)	Modeler (cm ³)	Support (cm ³)	Total (cm ³)	Estimated building time
Maching	1	Flat	Solid	20	260.082	2.54	262.622	4 h 6 min
	2	Edge	Solid	20	258.87	1.963	260.833	4 h 13 min
	3	Flat 45°	Solid	20	286.312	286.312	572.624	18 h 13 min
	4	Flat	Solid	15	131.567	1.596	133.163	2 h 12 min
	5	Edge	Solid	15	131.501	1.363	132.864	2 h 15 min
	6	Flat 45°	Solid	15	151.231	69.855	221.086	12 h 35 min
	7	Flat	Solid	10	53.736	0.873	54.609	59 min
	8	Edge	Solid	10	53.968	0.873	54.841	1 h
	9	Flat 45°	Solid	10	68.132	35.452	103.584	8 h 7 min
Hole printed	10	Flat	Sparse	20	16.358	0.329	16.687	38 min
	11	Edge	Sparse	20	18.789	6.196	24.985	2 h 3 min
	12	Flat 45°	Sparse	20	22.334	13.898	36.232	3 h 47 min
	13	Flat	Sparse	15	9.858	0.254	10.112	26 min
	14	Edge	Sparse	15	12.02	4.087	16.107	1 h 33 min
	15	Flat 45°	Sparse	15	14.562	9.21	23.772	2 h 45 min
	16	Flat	Sparse	10	5.091	0.19	5.281	18 min
	17	Edge	Sparse	10	6.914	2.517	9.431	1 h 6 min
	18	Flat 45°	Sparse	10	8.421	5.509	13.93	1 h 50 min

theoretical value that would appear in a hole, whose standard deviation would be acceptable around 1 mm between the top and bottom. In the absence of a specific standard for polymers, the criteria for permissible tolerances for metalworking were followed. Finally, measurements were made on the outer faces of all models. In that case, the values were taken at three heights on each front and for each volume.

3.5 Geometric deviations

One of the hypotheses previously stated is that, due to dilatation and contractions, the machining could introduce some thermal impact that would end up affecting the geometry of the models. To verify this hypothesis, the flatness of the three models' outer faces with a diameter of 20 mm was measured for both strategies. Additionally, to investigate the effect of the infill on flatness, two flat samples were manufactured with identical geometry as the printed specimen with a 20 mm hole, but with a sparse filler and a solid filler.

Nine measurements were made on each specimen: six along the length and the remaining three from top to bottom. Figure 4 includes an illustrative diagram of the different measurements and trajectories. A displacement LVDT probe [2] was used to measure the surface flatness, which was placed on the same milling machine to ensure movement at a constant speed. Measurements obtained correspond to the deviations of the dimension along the trajectories on the samples' surface in the orientations indicated above.

3.6 Roughness measurements

The roughness was measured in each hole, machined and FDM printed, by using a rugosimeter [3] with a range of 400 μm . The measurement was conducted following ISO 4287:1997 (1997) and UNE-EN ISO 12085:1998 (1998). To have a representative mean value of roughness, 10 measurements were made at different points on each hole. The high number of measures was very relevant, mainly in machined holes where the drill's action was very different along the trajectory. The data obtained are the arithmetic average roughness R_a and the total range roughness R_z , as well as the graphical representation of the profile before and after filtering.

3.7 Microscope imaging

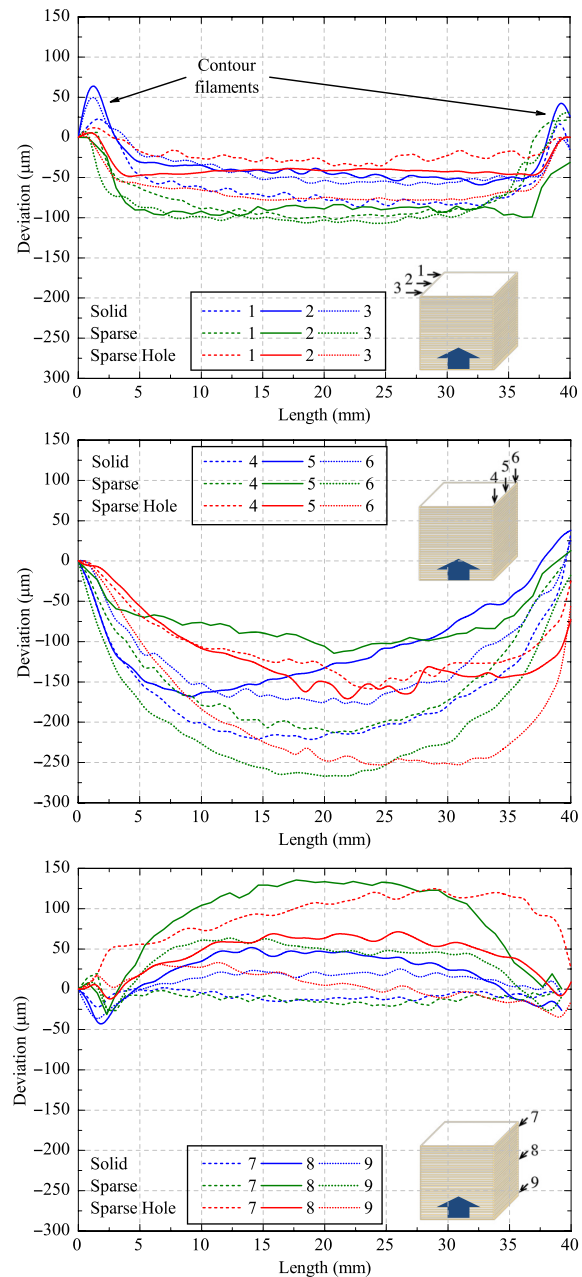
The specimens were analyzed under an optical and scanning electron microscope [4] (SEM) to have a better understanding of the results and to search for differences that were not perceptible before. First, upper and lower surfaces were examined to recognize the impact of the drill bit on the layers and their bond when machining, and in the FDM holes to analyze the area where the contour and raster merge. Second, $\phi 10$ mm diameter samples were segmented axially and analyzed by using the SEM along the hole. One specimen was inspected for each feed.

4. Results and discussion

4.1 Dimensional tolerances

The results obtained by the use of the go/no-go gauges are clarifying. As the tolerance range recommended by the printer manufacturer was so wide, in all combinations, both calibers met their measuring conditions, as expected. This occurred for

Figure 4 Deviations of the flatness measurement along the sides of printed specimens with different configurations



both strategies, i.e. printed and machined holes. As an example, the values corresponding to the measurement of the $\phi 20$ mm diameter holes are shown in Table 4. It should be noted that the condition of $\pm 0.3\text{mm}$ is never exceeded. The holes of the smallest diameters show the same tendency. An increase in cutting speed seems to increase the diameter of the holes. This may be caused by the relation between cutting speed and temperature increasing in the cutting zone. Nevertheless, it can be observed that hole diameter remains inside the tolerance zone, although for the highest cutting speed, they are only slightly above the nominal dimension.

Table 4 Measurements (in mm) for the $\phi 20$ mm diameter holes

Specimens	Feed	Cutting speed	Flat		Edge		45°	
			ϕ	σ	ϕ	σ	ϕ	σ
Maching	A1	V1	19.93	0.15	19.87	0.12	19.88	0.06
		V2	19.99	0.11	19.95	0.05	19.96	0.06
		V3	20.03	0.18	20.06	0.11	20.05	0.17
	A2	V1	19.92	0.18	19.96	0.13	19.96	0.13
		V2	19.98	0.13	19.91	0.07	19.92	0.08
		V3	20.03	0.15	20.04	0.07	20.06	0.04
	A3	V1	19.91	0.17	19.95	0.17	19.93	0.10
		V2	19.90	0.16	19.95	0.08	19.94	0.09
		V3	20.05	0.06	20.04	0.06	20.06	0.09
FDM-printed holes	-	-	19.83	0.07	19.81	0.17	19.80	0.03

However, by deeply analyzing the results, it can be seen that in machined specimens, all the holes are below the nominal dimension of the drill bit (diameter $\phi 20$ mm), except those that were machined at maximum speed (V3), regardless of the feed. This evidence reinforces the hypothesis that during the drilling process, the temperature generated in operation produces the dilatations and contractions of the polymer. Hence, the results prove that there is a critical speed for drilling, above which the hole exceeds the desired dimension.

In the checks done with the FDM-printed hole samples, the behavior is similar, except for the parts printed at 45°, in which the hole deviates considerably from the nominal dimension. In this case, the practical dimension is 0.2 mm, below the nominal dimension of the drill bit. This fact could be critical if the dimensional tolerance conditions the assembly with other parts. This phenomenon may be because the unique configuration where the contour is set around the hole is in a flat orientation. Thus, this printed contour makes the entire geometry much more regular. However, if the part is printed in the edge or 45° orientation, this delimitation cannot be accomplished, so two things are likely to happen. First, it would be necessary to place support material inside the hole, and this could affect not only the surface quality but also the dimensional quality. Second, during the material deposition in every 45° layers, the filament reaches the edge of the hole at a different angle. This fact could influence the homogeneity of the ends of these paths and, hence, the hole's final dimensional configuration. This phenomenon can be seen in [Figure 9](#). Based on a different analysis, these results could be aligned with those obtained by [Vijay et al. \(2011\)](#), who found a direct proportionality relationship between roughness and layer thickness at 45°. In this case, the trajectory changes that occur just in the contour generate variable thicknesses and higher than the rest of the piece [[Figure 9\(c\)](#)].

In summary, it could be stated that when holes are machined in printed parts, the cutting speed must be controlled when the final dimension conditions the viability of the assembly. In contrast, when holes are printed directly on the specimen, the building orientation conditions the final dimension.

In addition to the holes, the outer dimensions of the specimens were also measured. In none of the two study conditions, it was found that the final measurements exceeded the expected ± 0.3 mm interval. However, it should be noted

that the results show high variability depending on the measurement location. Although the values are below the nominal height, the measures taken at the extremes are significantly different from those measured in the central parts. In almost all cases, a sink-in in the center is identified. To analyze more accurately the effect of these deviations, flatness measurements were also carried out, which are discussed in the next section.

4.2 Geometric deviations

Infill density is a characteristic parameter between machined parts and non-machined parts. For machining, a 100% infill was needed. Otherwise, gaps would be found in the hole. In FDM-printed holes, a sparse infill (50%) was applied to take advantage of two primary benefits of additive manufacturing: saving time and material. However, these sparse specimens show a visible alteration of the flatness at their external faces ([Figure 1](#)), being, thus, necessary to quantify the effect of the infill density on the flatness of the outer surfaces. The possibility of this phenomenon was already foreseen when analyzing the work by [Ituarte et al. \(2015\)](#). This study showed that, regardless of the AM technology used, surface quality and flatness were precisely two of the most difficult challenges to achieve with these technologies.

The graphs depicted in [Figure 4](#) represent the deviation of the dimension along the paths defined in the diagrams. By visual inspection, differences were observed between the ends and the center of the samples or between the outer contours and the area around the holes, which did not meet a regular criterion. Accordingly, three measurement positions were taken. The results correspond to three flat specimens with different fillers: solid, sparse and spare with a 20 mm hole. Although the trends are similar for the three specimens, there are significant differences in the different planes.

A minor shrinkage deviation is observed on the upper face, with a slight difference between the three configurations. The initial and final perturbations correspond to the contour filaments. However, on the vertical side and in the building direction, a remarkable contraction of up to 250 μm is observed. The most significant deviation corresponds to the external trajectories (4 and 6) in all three configurations. On the contrary, in the horizontal direction of the vertical face, a dilatation is observed for all configurations. The initial disturbance corresponds to the coincidence of the beginning of the trajectory of each layer.

The shrinkage deviation is attributable to the thermal impact of the manufacturing process, together with the influence of the infill that introduces changes in the way in which the material is distributed and solidified inside, to the point that the outer dimensions are affected. Consequently, the infill role is something to take into consideration if the FDM printed parts must guarantee strict geometric relationships with other components in the assemblies. In any case, these effects should not introduce dramatic dimensional modifications, considering that the specimens have been printed on a Fortus 400mc. This professional printer maintains the temperature of the printing environment stable throughout the process. However, as the origins and ends of the printing paths are random, and the time it takes for one layer to overlap on the previous one is not

constant, the influence on the dimensions of these thermal effects cannot be ruled out.

In the results of the mechanized samples, no significant modification of the geometric deviations of the plane surfaces surrounding the machined holes is observed due to possible expansions and contractions during drilling. In other words, the possible thermal expansion caused by the heating of the drill bit did not affect the external dimensions of the specimens when they were printed. Accordingly, the hypothesis stated above is discarded, getting viable the machining of FDM printed parts.

4.3 Roughness measurements

The values obtained of the roughness indicators R_a and R_t for all test conditions considering all the parameters under study are grouped in Table 5.

The overview of results confirms the hypothesis that models in which the hole was machined presented better surface quality than the printed holes. As can be seen in Table 5, the cutting speed becomes the critical parameter again. As the cutting speed increases, the roughness worsens considerably, with the interval between V2 and V3 being very pronounced. Concerning the feed, it does not seem to exert a determining influence on the results, nor does the direction of construction in none of the strategies. To confirm these assumptions, two Pareto graphs are depicted in Figure 5. The significance for both R_a and R_t can be appreciated. The rest of the technological parameters do not exert any significant influence on the roughness measured inside the holes.

The degree of influence of each parameter can be examined in more detail, analyzing the main effects graph represented in

Table 5 Roughness measurement results for all configurations under study

Specimens	Feed rate	Cutting speed	Flat		Edge		45°	
			R_a	R_t	R_a	R_t	R_a	R_t
Maching	A1	V1	0.88	6.22	0.86	8.65	1.11	13.63
		V2	1.82	12.79	1.46	16.63	3.36	33.46
		V3	5.08	35.82	3.92	31.35	6.11	38.85
	A2	V1	0.60	4.89	1.26	15.08	0.90	7.74
		V2	1.54	14.98	0.94	11.29	1.21	15.18
		V3	5.35	39.37	3.61	27.32	4.24	34.96
	A3	V1	0.71	6.11	1.01	9.38	1.15	14.24
		V2	1.80	20.54	1.09	15.54	1.02	11.00
		V3	3.18	24.24	2.96	31.36	1.69	19.84
FDM	-	-	20.81	85.98	3.83	20.22	29.52	122.49

Figure 5 Pareto diagram for R_a and R_t

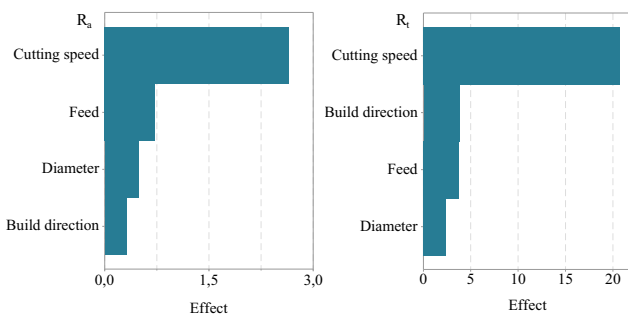
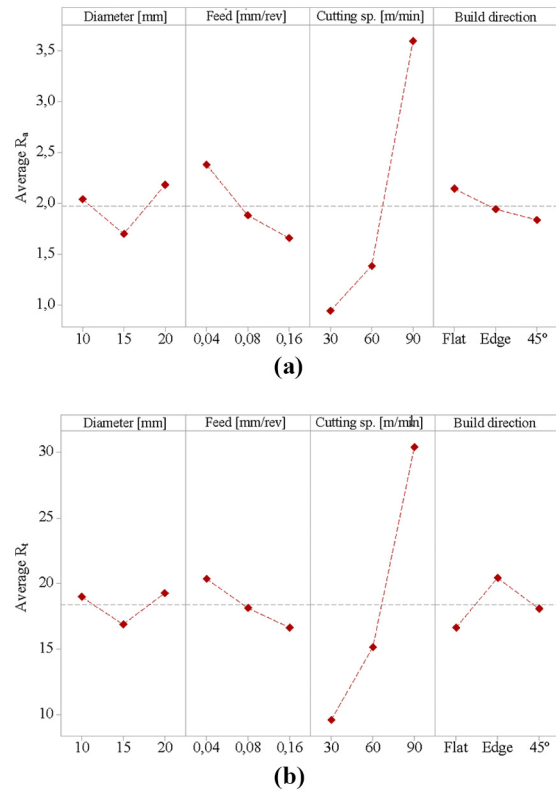


Figure 6. In the case of R_a , it is confirmed that there is a directly proportional relationship between roughness and cutting speed, that the feed is inversely proportional and that the best construction orientation is 45°. This same trend is also true for the main effects of R_t .

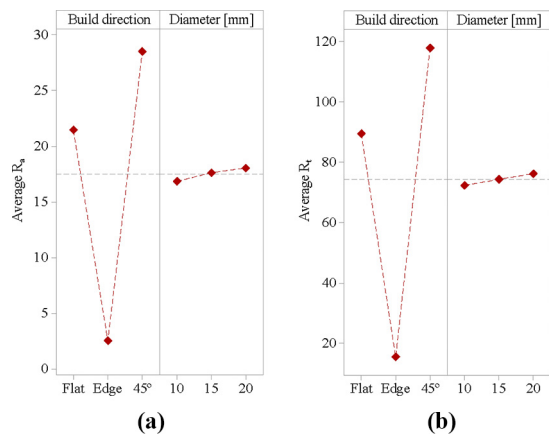
The roughness obtained on FDM-printed parts, although worse, is also the result of the combination of printing parameters. Figure 7 shows the results in the main effects graph.

Figure 6 R_a and R_t effect according to the standard deviation of the machined holes



Notes: (a) Main effects for R_a ; (a) main effects for R_t

Figure 7 R_a and R_t effect according to the standard deviation of the printed holes



Notes: (a) Main effects for R_a ; (a) main effects for R_t

For both R_a and R_p , the best values were obtained in the edge building orientation, while the worst results are at 45° . In this case, the diameter does not reveal any significance. If the roughness results of the outer faces were compared with those obtained inside the hole, the statements of Pandey *et al.* (2003) are corroborated, who agree that the more intricate the areas manufactured by AM, the greater the probability of the surface quality worsening, even when they use of support material is not necessary.

Finally, in Figure 8, the diagram is shown with the deviation of the data for each parameter combination for both R_a and R_p . It can be corroborated that the higher cutting speed generates, the more significant deviation, as has been demonstrated. Previously, it was considered that the hole diameters' influence is not significant; consequently, it has been excluded from the results.

4.4 Microscope imaging

To observe the structural singularities of the building orientation, images of the filament distribution were taken with an optical microscope in the specimens with the printed hole (Figure 9).

As can be seen, the flat orientation [Figure 9(a)] is the only one in which a contour is deposited around the hole, which imposes a certain precision in the delimitation of the layers and consequently, in the quality of the interior surface. When printing on the edge orientation [Figure 9(b)], the distribution of the filaments shows that it is necessary to place support material inside and the same happens when printing at 45° [Figure 9(c)], where the definition of the boundary of the layer is even more diffuse. For that reason, two factors prevent a satisfactory surface finish: the arrangement of the layers and the extraction of the support material adhered to the surface, which also has an impact on the result.

On the other hand, to visually evaluate the velocity behavior concerning the final roughness of the mechanized specimens,

Figure 8 Interval plot for R_a and R_p (95% confidence interval)

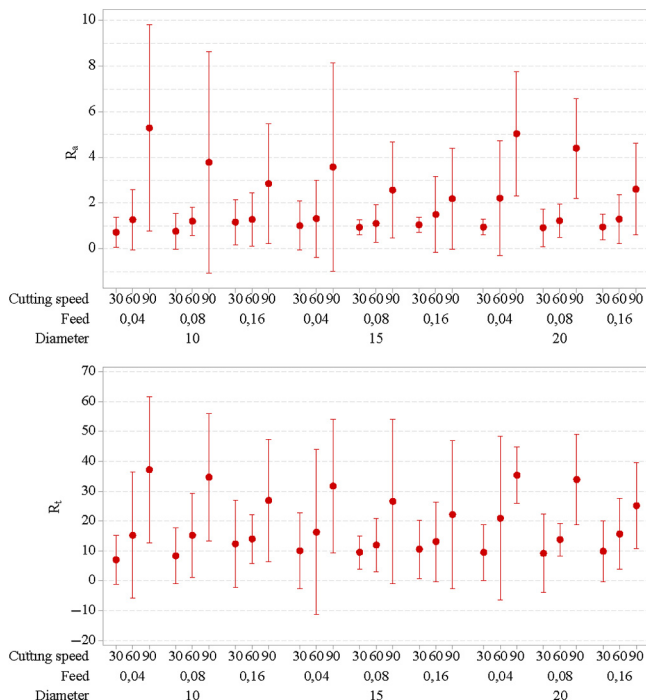
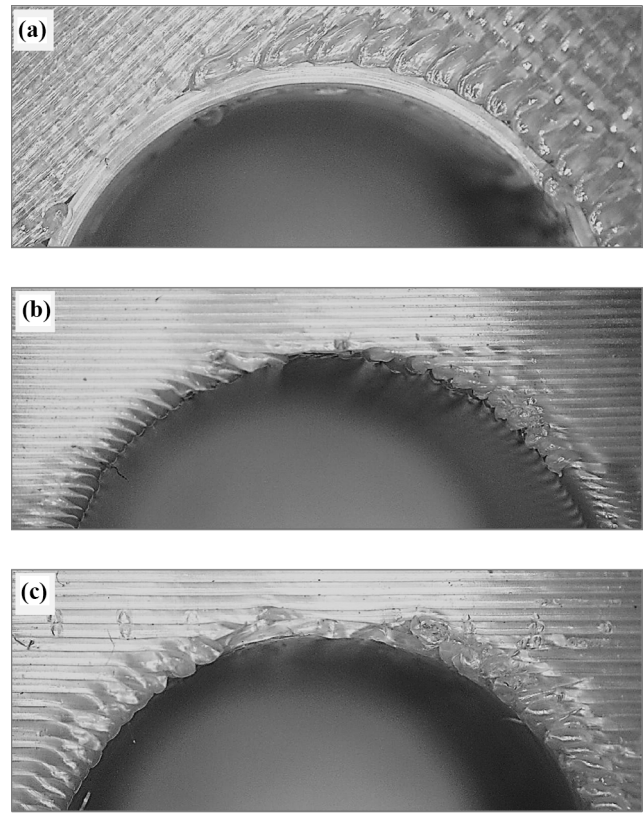


Figure 9 Images obtained by light field optical microscope

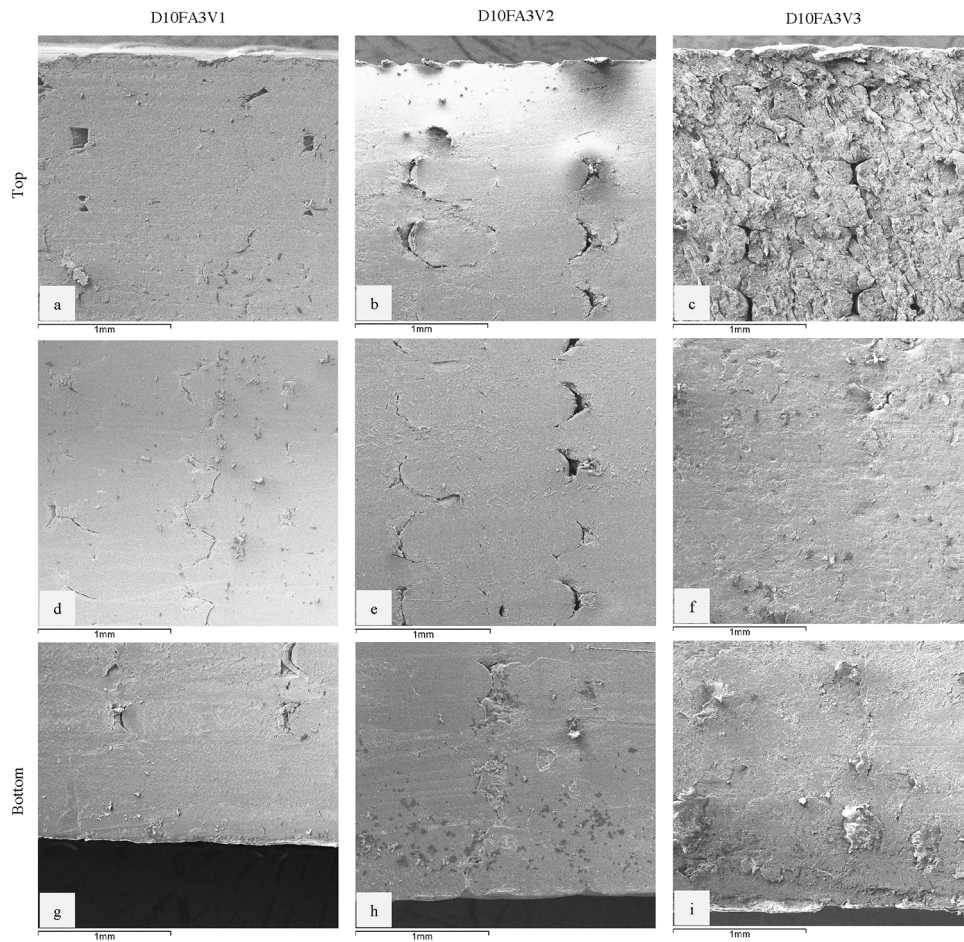


Notes: (a) Top surface for flat orientation specimen; (b) top surface for edge orientation specimen; (c) top surface for 45° orientation specimen

the 10 mm diameter specimens D10FA3V1, D10FA3V2 and D10FA3V3 were examined. These specimens were analyzed by using the SEM, capturing consecutive images at three heights, from top to bottom in the direction of bit penetration into the part (Figure 10).

The microscopic examination corroborates the same results previously obtained. At high cutting speeds, the roughness worsens. The hypothesis that could explain these results is related to the thermal variations that occur during machining. The roughness at the top is higher, because the drill bit is entering the part and, as the temperature increases with penetration, the filament stop cutting and start to melt and be dragged by the thermal change itself. In the bottom part, a lower roughness is obtained, as the machining is a mixture between the cut and the melting effect introduced by the temperature.

In other words, considering that the feed is the same in all three cases, as the cutting speed increases, the dwell time of the drill inside the hole decreases accordingly. Therefore, these higher cutting speed values also increase the feed, leaving a poor quality surface on top (i.e. less exposure time to machining). This combination of parameters also generates an increase in temperature in the cutting area, causing the intermediate height filaments to melt and improve the finish locally. The visual effect can be seen in the images in Figure 10(c), 10(f) and 10(i), where the changes between top and bottom are more pronounced. This

Figure 10 Images obtained by SEM. From left to right the cutting speed increases

Notes: From top to bottom the through-thickness sections are shown

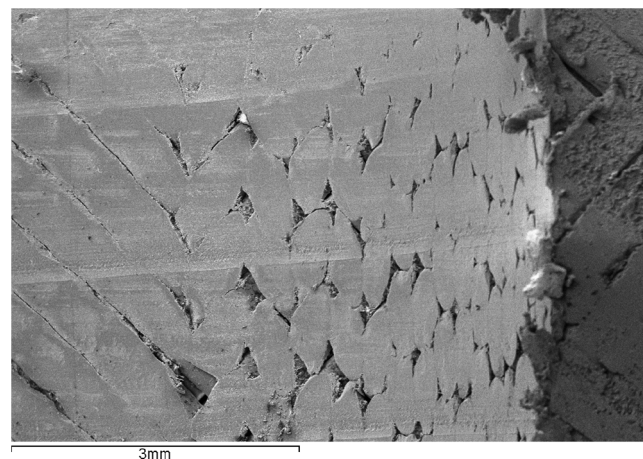
evidence corroborates why a significant increase in cutting speed results in a less uniform surface.

By analyzing the images obtained by the SEM, some features can be appreciated. For example, a remarkable detail was revealed when observing the machined holes in the pieces printed at 45° (Figure 11). In a left-hand section of the hole, the raster of the adjacent layers melted, leaving V-shaped marks on the machined surface, while on the right-hand side, due to the filament's position, the weft changes completely. In this case, the filaments cross perpendicular to the direction of rotation of the drill bit, so that, when machining them, the cut ends of the threads can be appreciated. This makes it possible to ensure that the surface roughness is not homogeneous on parts that have been printed at 45° . For the flat-build orientation specimens, this phenomenon is not appreciated.

5. Conclusions and recommendations

Once analyzed and discussed all the experimental results previously exposed, it has been possible to reach the following conclusions:

- Concerning the volume material and manufacturing time, the most optimal configuration is the flat build orientation and sparse filling.

Figure 11 SEM image detail of the machined hole of the specimen D1045A3V2 printed at 45° 

- Experimental evidence reveals that, among the tested scenarios, the best parameter combination for minimizing R_a and R_z values is 30 m/min cutting speed (lowest value), 0.16 mm/rev feed (highest value) and flat build

orientation. It should be noted that the feed does not introduce relevant changes in roughness.

- Best R_a result obtained was $0.4217 \mu\text{m}$ and the best R_t result was $2 \mu\text{m}$.
- The most influencing parameter was the cutting speed, which had a reversely proportional relation with R_a and R_t results. The diameter and build direction showed the least influence in roughness results.
- The temperature turned out to be a relevant parameter regarding the machining process. Depending on the parameter level selection, the surface filaments were melted during the drilling, providing a better result concerning roughness.
- From SEM images, additionally to the temperature findings, it was found that the raster interjects differently with the hole along the surface, thus bringing more significant variation in results.

Accordingly, for industrial use, the recommendations to be considered for obtaining printed parts by FDM of Ultem, in which holes are present with specific geometric and dimensional tolerances are:

- To print the parts on flat orientation and sparse infill, with a previous hole with a nominal dimension smaller than the final dimension, as this saves material and manufacturing time. Moreover, the number of contours must be related to the amount of material to be removed by the drill. The advantages of sparse printing are widely explained in Forés-Garriga et al. (2020).
- If it is to be adjusted, the final hole dimension must be obtained by machining, as the results of surface roughness and dimensional tolerances are significantly better. The smaller the amount of material removed by the drill, the less chance that the thermal effect will damage the contours.
- When selecting the machining parameters, the cutting speeds should be low. The changes concerning the feed are not particularly significant, except when combined with the cutting speed, in which case an increase in the feed would result in non-uniform surfaces.

A further line of research focuses on the development of thermochemical post-processing to guarantee lower roughness values, facilitating assembly with parts of other materials and contributing to the improvement of geometric and dimensional tolerances.

Notes

1. Drills Guhring DIN 338 N HSS.
2. HBM WI 5 mm.
3. Rugosurf 20 TESA Technology.
4. Jeol Electron Microscope JSM 5310.

References

- Anitha, R., Arunachalam, S. and Radhakrishnan, P. (2001), "Critical parameters influencing the quality of prototypes in fused deposition modelling", *Journal of Materials Processing Technology*, Vol. 118 Nos 1/3, pp. 385-388.
- Bahrami, B., Ayatollahi, M.R., Sedighi, I., Pérez, M.A. and Garcia-Granada, A.A. (2020), "The effect of in-plane layer

orientation on mixed-mode I-II fracture behavior of 3D-printed poly-carbonate specimens", *Engineering Fracture Mechanics*, Vol. 231.

- Chang, D.Y. and Huang, B.H. (2011), "Studies on profile error and extruding aperture for the rp parts using the fused deposition modeling process", *The International Journal of Advanced Manufacturing Technology*, Vol. 53 Nos 9/12, pp. 1027-1037.
- Chohan, J.S. and Singh, R. (2017), "Pre and post processing techniques to improve surface characteristics of fdm parts: a state of art review and future applications", *Rapid Prototyping Journal*, Vol. 23 No. 3, pp. 495-513.
- Chueca de Bruijn, A., Gómez-Gras, G. and Pérez, M.A. (2020), "Mechanical study on the impact of an effective solvent support-removal methodology for FDM ultem 9085 parts", *Polym. Test*, Vol. 85.
- Del Sol, I., Domínguez Calvo, Á., Piñero, D., Salguero, J. and Batista, M. (2019), "Study of the fdm parameters of the abs parts in the surface quality after machining operations", *Key Engineering Materials*, Vol. 813, pp. 203-208.
- Fernandez-Vicente, M., Calle, W., Ferrandiz, S. and Conejero, A. (2016), "Effect of infill parameters on tensile mechanical behavior in desktop 3D printing", *3D Printing and Additive Manufacturing*, Vol. 3 No. 3, pp. 183-192.
- Ford, S. and Despeisse, M. (2016), "Additive manufacturing and sustainability: an exploratory study of the advantages and challenges", *Journal of Cleaner Production*, Vol. 137, pp. 1573-1587.
- Forés-Garriga, A., Pérez, M.A., Gómez-Gras, G. and Reyes-Pozo, G. (2020), "Role of infill parameters on the mechanical performance and weight reduction of PEI ultem processed by FFF", *Mater. Des*, Vol. 193.
- Galantucci, L., Lavecchia, F. and Percoco, G. (2009), "Experimental study aiming to enhance the surface finish of fused deposition modeled parts", *CIRP Annals*, Vol. 58 No. 1, pp. 189-192.
- Galantucci, L., Lavecchia, F. and Percoco, G. (2010), "Quantitative analysis of a chemical treatment to reduce roughness of parts fabricated using fused deposition modeling", *CIRP Annals*, Vol. 59 No. 1, pp. 247-250.
- ISO 4287:1997 (1997), *Geometrical Product Specifications (GPS) – Surface Texture: Profile Method. Terms, Definitions and Surface Texture Parameters*, International Organization for Standardization (ISO).
- Iuarte, I.F., Coatanea, E., Salmi, M., Tuomi, J. and Partanen, J. (2015), "Additive manufacturing in production: a study case applying technical requirements", *Physics Procedia, 15th Nordic Laser Materials Processing Conference, Nolamp 15*, Vol. 78, pp. 357-366.
- Mohamed, O.A., Masood, S.H. and Bhowmik, J.L. (2015), "Optimization of fused deposition modeling process parameters: a review of current research and future prospects", *Advances in Manufacturing*, Vol. 3 No. 1, pp. 42-53.
- Mohamed, O.A., Masood, S.H. and Bhowmik, J.L. (2017), "Experimental investigation of time-dependent mechanical properties of PC-ABS prototypes processed by fdm additive manufacturing process", *Materials Letters*, Vol. 193, pp. 58-62.

- Nidagundi, V., Keshavamurthy, R. and Prakash, C. (2015), "Studies on parametric optimization for fused deposition modelling process", *Materials Today: Proceedings, 4th International Conference on Materials Processing and Characterization*, Vol. 2 Nos 4/5, pp. 1691-1699.
- Nunez, P., Rivas, A., García-Plaza, E., Beamud, E. and Sanz-Lobera, A. (2015), "Dimensional and surface texture characterization in fused deposition modelling (FDM) with ABS plus", *Procedia Engineering, MESIC Manufacturing Engineering Society International Conference 2015*, Vol. 132, pp. 856-863.
- Pandey, P.M., Reddy, N.V. and Dhande, S.G. (2003a), "Improvement of surface finish by staircase machining in fused deposition modeling", *Journal of Materials Processing Technology*, Vol. 132 Nos 1/3, pp. 323-331.
- Salazar-Martín, A., Pérez, M.A., García-Granada, A.A., Reyes, G. and Puigoriol-Forcada, J. (2018), "A study of creep in polycarbonate fused deposition modelling parts", *Mater. Des.*, Vol. 141.
- Sedighi, I., Ayatollahi, M.R., Bahrami, B., Pérez, M.A. and Garcia-Granada, A.A. (2019), "Mechanical behavior of an additively manufactured poly-carbonate specimen: tensile, flexural and mode I fracture properties", *Rapid Prototyping Journal*, Vol. 26 No. 2, pp. 267-277.
- Singh, R., Singh, S., Singh, I.P., Fabbrocino, F. and Fraternali, F. (2017), "Investigation for surface finish improvement of fdm parts by vapor smoothing process", *Composites Part B: Engineering*, Vol. 111, pp. 228-234.
- Sood, A., Ohdar, R. and Mahapatra, S. (2010), "Parametric appraisal of mechanical property of fused deposition modelling processed parts", *Materials & Design*, Vol. 31 No. 1, pp. 287-295.
- Tiwary, V.K., Arunkumar, P., Deshpande, A.S. and Rangaswamy, N. (2019), "Surface enhancement of fdm patterns to be used in rapid investment casting for making medical implants", *Rapid Prototyping Journal*, Vol. 25 No. 5, pp. 904-914.
- UNE-EN ISO 12085:1998 (1998), *Geometrical Product Specifications (GPS) – Surface Texture: Profile Method – Motif Parameters*, International Organization for Standardization (ISO).
- Vasudevarao, B., Natarajan, D.P. and Henderson, M. (2000), "Sensitivity of Rp surface finish to process parameter variation", *Solid Freeform Fabrication Proceedings*, pp. 251-258.
- Vijay, P., Danaiah, P. and Rajesh, K.V.D. (2011), "Critical parameters effecting the rapid prototyping surface finish", *Journal of Mechanical Engineering and Automation*, Vol. 1 No. 1, pp. 17-20.
- Wang, J., Xie, H., Weng, Z., Senthil, T. and Wu, L. (2016), "A novel approach to improve mechanical properties of parts fabricated by fused deposition modeling", *Materials & Design*, Vol. 105, pp. 152-159.
- Zandi, M.D., Jerez-Mesa, R., Lluma-Fuentes, J., Roa, J. and Travieso-Rodriguez, J.A. (2020), "Experimental analysis of manufacturing parameters' effect on the flexural properties of wood-PLA composite parts built through FFF", *The International Journal of Advanced Manufacturing Technology*, Vol. 106 Nos 9/10, pp. 3985-3998.

Corresponding author

Marco A. Pérez can be contacted at: marcoantonio.perez@iqs.edu